Double Mobility: Coverage of the Sea Surface with Mobile Sensor Networks

Ji Luo
Hong Kong Univ. of Science and Tech.
luoji@cs.ust.hk

Dan Wang
Hong Kong Polytechnic Univ.
csdwang@comp.polyu.edu.hk

Qian Zhang
Hong Kong Univ. of Science and Tech.
qianzh@cs.ust.hk

***Abstract*—We are interested in the sensor networks for scientific applications to cover and measure statistics on the sea surface. Due to flows and waves, the sensor nodes may gradually lose their positions; leaving the points of interest uncovered. Manual readjustment is costly and cannot be performed in time. We argue that a network of mobile sensor nodes which can perform self-adjustment is the best candidate to maintain the coverage of the surface area.**

In our application, we face a unique *double mobility* coverage problem. That is, there is an uncontrollable mobility, U-Mobility, by the flows which breaks the coverage of the sensor network. Moreover, there is also a controllable mobility, C-Mobility, by the mobile nodes which we can utilize to reinstall the coverage. Our objective is to build an energy efficient scheme for the sensor network coverage issue with this double mobility behavior.

A key observation of our scheme is that the motion of the flow is not only a curse but should also be considered as a fortune. The sensor nodes can be pushed by free to some locations that potentially help to improve the overall coverage. With that taken into consideration, more efficient movement decision can be made. To this end, we present a dominating set maintenance scheme to maximally exploit the U-Mobility and balance the energy consumption among all the sensor nodes. We prove that the coverage is guaranteed in our scheme. We further propose a fully distributed protocol that addresses a set of practical issues. Through extensive simulation, we demonstrate that the network lifetime can be significantly extended, compared to a straight forward back-to-original reposition scheme.

I. Introduction

Sensor networks today are penetrating into people's life in a stunting speed. The capabilities of the sensor nodes have gone broader beyond a static sensing device; and now they include mobility, communication, computation, etc. They provide valuable information that is originally difficult or impossible to obtain in all domains. To name a few, we have recently seen the design and deployment of applications such as the structural health monitoring for roads and bridges [14], monitoring of ecological systems (e.g., redwood trees), measurement and data collection of active volcanos [7].

In this paper, we are interested in applications which need to collect data in an area of interest on the sea surface. The data are valuable in many aspects. For scientific applications, the measurement of salt level at the mouth of a glacier can serve a good indicator for the melt speed during different seasons. For recreation purposes, the temperature and wave strength of the sea may help divers to choose better locations and prepare equipments. Clearly, we need to have the area monitored for these applications. It is therefore efficient to deploy some sensor nodes floating on the sea surface to form a sensor network that covers the area and reports the data.

The coverage issue for sea surface monitoring applications is challenging and in sharp contrast to static sensor coverage problems, as the sensor nodes face the continuous motion of the flows and waves. In some existing applications, drifters and moorings are used to build the sensor network [1] for water surface monitoring. If unattended, a drifter [2] cannot keep its position; thus not suitable for monitoring a fixed area. A mooring [4] is anchor at the sea bottom and is able to stay put. The deployment, however, is usually more complicated and requires professional technicians. In addition, it is restricted in shallow waters only. These solutions are thus not adequate to achieve an autonomous coverage for sea surface monitoring sensor networks.

We consider sensor nodes with movement capability to be the best candidate to form the sensor network for our applications. Some existing studies have used mobile sensor nodes to assist area coverage on land. We are different, however, as we face a *double mobility* coverage problem. On one hand, the sensor nodes will be affected by the motion of flows and waves. They will gradually lose their positions. This mobility is uncontrollable (we call it *U-Mobility* thereafter) and the coverage of the sensor network may be broken by the U-Mobility. On the other hand, the mobile sensor nodes have the movement capability to reinstall the network coverage. This mobility is controllable (we call it *C-Mobility* thereafter).

The sensor nodes are battery powered and the most stringent resource is energy. In our application, the sensor network has to monitor the area of interest for a long period of time. If the battery of a sensor node is depleted, a manual battery replacement by sending a technician is expensive. Thus, the frequency of this operation should be minimized. For the mobile sensor nodes, the dominant factor of the energy consumption is the mechanical movement, i.e., the C-Mobility. Consequently, the objectives of our system include 1) the sensor nodes should collaboratively monitor and guarantee coverage of the area of interest; 2) the movement of the sensor nodes due to C-Mobility should be minimized and the power consumption should be balanced in the long run; and 3) the sensor network should be able to adapt to different U-Mobility patterns; as there is no universal U-Mobility model that can capture the behavior of all sea.

We achieve the aforementioned objectives by considering the interaction between the U-Mobility and the C-Mobility. Our key observation is that the U-Mobility should not only be considered as a curse that the C-Mobility should always counter-effect, but also a fortune. With U-Mobility, some

sensor nodes may be pushed to positions that may improve the coverage. Thus, less C-Mobility is needed if taking this into consideration. We first discuss two general yet realistic U-Mobility models, namely, the meandering current model [8] and a random ring model [3] which may capture the mobility of different water bodies. Our C-Mobility is designed in a way such that it can fit for different U-Mobility models. In our C-Mobility scheme, each sensor node dominates (maintains) a set of points that it covers; and the sensor network dominates all the points of interest. We design a distributed event driven algorithm to maintain the coverage. When a point of interest is not covered, the algorithm finds a substitute by a joint optimization with consideration of the velocity constraints of the sensor nodes, the balance of power consumption and maximizing the advantage of U-Mobility. A low-overhead protocol is designed thereafter which addresses a set of practical difficulties such as collisions and local inconsistent views of the sensor nodes introduced by the distributed algorithm. We prove that the coverage is guaranteed based on our scheme. Extensive simulations have shown that our scheme significantly outperforms a straightforward back-to-original scheme for different U-Mobility models under various configurations.

As a summary, the contributions of the paper are 1) We are the first to address the coverage issue for the double mobility scenario. We provide key observation that although U-Mobility brings significant challenge, we can also leverage it to solve the coverage issue in a more efficient way. 2) We formulate the double mobility problem, and propose a distributed dominating set maintenance approach to solve it. 3) We propose a practical distributed protocol and conduct comprehensive simulation which verifies the effectiveness of the proposed scheme.

The remaining part of the paper proceeds as follows. Section II presents the related work. An overview of the system design and challenges is presented in Section III. We discuss the U-Mobility models in Section IV. Section V is devoted to the design and optimization of the detailed sea surface coverage solutions. Protocol specifications are described in Section VI. We evaluate the performance of the system in Section VII; and finally Section VIII concludes the paper.

II. Related Work

Sensor network today has been applied to many applications for data collection on land [15][20]. Collecting data to better understand the sea, though also important, is far lagging behind. Currently some data of the sea are captured by the satellites [5]. These data, however, usually provide a macro view of a large geographic region during a long period of time; without the details that are suitable for applications that request for micro level data. Using sensor networks is consider to be a feasible and effective solution for these applications. Nevertheless, such difficulties as deployment, communication, etc., need to be addressed; see comprehensive research challenges in [6]. Providing effective coverage is among them before bringing these applications into reality.

Most of the existing works related to coverage issue in sensor networks are focus on static sensor nodes [15]. For the sea surface monitoring applications, significant reconsideration is needed as the motions of the flows and waves will push the sensor nodes away from their positions.

The motion of the sea flows and waves is affected by a number of factors [3], such as salt level, wind, temperature, geographic outlines and in water obstacles such as reefs [11]. In general, the sea flows can be approximated as a stochastic process. However, accurately modeling the water circulation is not an easy task. Especially, different sea or different regions of the sea may have different circulation patterns. Some current advances in oceanography can be found in [17]. There is a recent meandering current model for the underwater circulations [8] and captures the horizontal motion. In our paper, we will apply this model and propose a random ring model to capture the basic sea flow motion.

There are many studies that utilize mobile nodes with controllable mobility to assist or improve application performance. For sensor coverage issues, they can be classified into two main categories. First, hybrid architecture with both mobile and static sensor nodes is proposed to assist area coverage [9][21]. In these works, the mobile nodes move to fix the coverage holes caused by the uneven distribution of the static sensor nodes. None of them faces the effect of U-Mobility, however. Second, there are sensor networks with mobile nodes only. The nodes are self-controlled to move continuously to improve the overall coverage [16]. Howard [13] proposed a moving scheme based on potential field to maximize the coverage. However, this work does not guarantees full coverage; and again it does not face the U-Mobility.

In all these works, none of them faced the double mobility scenario as in this paper, where the interaction between the U-Mobility and the C-Mobility should be carefully considered.

III. The Problem and Design Considerations

A. Problem Statement

Assume the region is composed of $m \times m$ cells. Let the set of points of interest be I, which is a subset of the cells of the region. There are N sensor nodes deployed in these cells to cover I. By convention, we use (px, py) to denote the cells in I; and (ox_i^t, oy_i^t) to denote the position of the sensor node i at time t. All sensor nodes have the same coverage capability and we use a disk coverage model with a sensing range of R_s. We assume that the time is divided into slots. For the applications that we are interested in, the data sampled at the same time is more useful for data analysis. Consequently, the sensor network has to sample the data periodically every T time slots. Thus, our definition of coverage is:

Definition 1: Given a time T, I should be covered every T time slots, i.e.,

$$\begin{aligned} &\forall k > 0, \forall (px, py) \in I, \exists\ sensor\ node\ i, \\ &s.t. \sqrt{(ox_i^{kT} - px)^2 + (oy_i^{kT} - py)^2} \leq R_s \end{aligned} \tag{1}$$

We assume that the sensor nodes have GPS or other facilities which can help them to obtain their positions and system time. The communication range of a sensor node is R_c.

In our application, the sensor nodes are initially deployed to provide full coverage of I by technicians. If the battery of a mobile sensor node is depleted, we will have to send a technician for battery replacement as the mobile sensor nodes (with scientific apparatus) can be expensive and the lost of the sensor node by the flows may even cause environmental issues. Due to the cost of dispatching the technician, the batteries of all the nodes will be replaced. Therefore, we use the first depleted sensor as a measurement of the system lifetime, which is also widely used in current research as an indication of the end of a steady-state operation.

To illustrate the double mobility of a mobile sensor node, let the velocity constraint for the U-Mobility be V_u, i.e., at every time slot, a sensor node can only be pushed to another cell that is at most V_u steps away (in the stochastic process, the probability that the sensor node will be moved farther than V_u in one time slot is zero). Let the velocity constraint for C-Mobility be V_c. Notice that we assume $V_c \geq V_u$. Otherwise, it is impossible to guarantee coverage.

Let $(U_x(x,y), U_y(x,y))$, $(C_x(x,y), C_y(x,y))$ denote the locations of a node, at (x,y), after U-Mobility and C-Mobility respectively. The location transformation of a node from t to $t+1$ can be represented as:

$$\begin{cases} ox^{t+1} &= C_x(U_x(ox^t, oy^t), U_y(ox^t, oy^t)) \\ oy^{t+1} &= C_y(U_x(ox^t, oy^t), U_y(ox^t, oy^t)) \end{cases} \quad (2)$$

Let the energy reserve for each node be $e^0 = max\_energy$ at time slot 0. At every time slot, C-Mobility consumes energy and is represented by the total steps the node travels:

$$\begin{aligned} e^{t+1} &= e^t - |C_x(U_x(ox^t, oy^t), U_y(ox^t, oy^t)) - U_x(ox^t, oy^t)| \\ &\quad -|C_y(U_x(ox^t, oy^t), U_y(ox^t, oy^t)) - U_y(ox^t, oy^t)| \end{aligned}$$

Notice that we ignore the energy cost of sensing and communication. As shown in [18], a typical mobile sensor node consumes 27.96 Joule per meter in moving whereas the energy consumption of transmission is in the order of 100×10^{-9} Joule per bit and sensing is even less [12]. Generally speaking, it is widely accepted that mechanical movement is much more energy expensive than electronic communications.

The sensor nodes could cover all cells of I at time slot 0. With U-Mobility, the objectives of C-Mobility are thus:

1) The coverage is guaranteed according to Definition 1,
2) Maximize the network lifetime L:

$$maximize\ L,\ s.t.\ \forall i \in N, e_i^L > 0 \quad (3)$$

B. Observations and Challenges

To have an energy efficient design for sea surface coverage, a key observation is that the U-Mobility not only drives the sensor nodes away and breaks the coverage of the sensor network; it also sends nodes to positions that may improve the coverage by free. The sensor nodes should take the advantage of this U-Mobility as much as possible.

Nevertheless, we faced many challenges in the design. First, the U-Mobility is a stochastic process whereas our application is looking for a deterministic full coverage every T time slots. Notice that even each step of the U-Mobility is known in advance, it is still a max-min problem that is NP-hard. Second, though we may neglect the time for algorithm computation and communication at sensor nodes, the velocity of the nodes has a limit. It is unrealistic to design a scheme that the sensor network conducts a re-optimization at the last time slot in each period of T time slots, and assume the nodes are able to hurry to the respective locations to cover I. Third, though we may explore the benefit of the U-Mobility, the coverage scheme should not depend on a specific U-Mobility model.

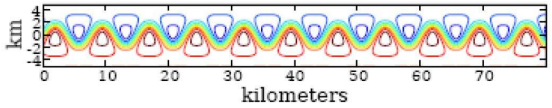

Fig. 1. A Plot of The Meandering Model at t = 0.

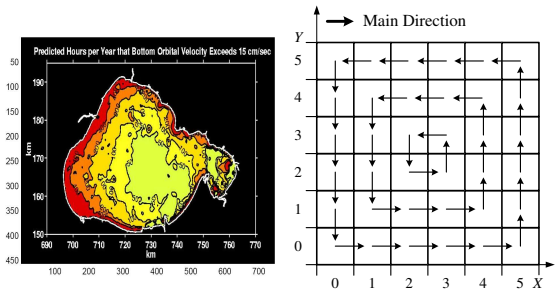

(a) The circulation of Lake Pontchartrain (b) An Example of Main Circulation

Fig. 2. Main Circulation of Lake Pontchartrain

In this paper, we take a fully distributed approach that every sensor node performs computation based on local information. Every node adjusts its status and may perform C-Mobility at every time slot, according to its estimation/optimization of the system parameters. We focus on period $[0, T]$; different periods in our approach are statistically identical.

A straight forward algorithm is a *back-to-original* scheme. Sensor node calculates its position in every single time slot within the period $[0, T]$. The node starts to move back to its original position at time $\Delta \in [0, T]$ given that after this time slot, there may not be enough time to return to the original position in the worst case. Apparently, this algorithm is not optimized as we will demonstrate in Section VII as U-Mobility has not been leveraged.

IV. The U-Mobility

Before going into our scheme, we first study the U-Mobility models. Modeling the sea flows is not an easy task. Due to wind, salinity, reefs, temperature, different sea has different circulation characteristics. In general, the sea flow can be considered as a stochastic process with both local variety (caused by reefs, turbulence), and the main circulation effects (caused by wind, salinity). By no means this paper provides a comprehensive study on modeling sea flows. We refer interested readers to [17]. In this paper, we will use two concrete models as examples to discuss the interaction between U-Mobility and C-Mobility.

In [8], a simplified model (meandering current model) is presented for underwater circulation. The mobility is divided into a fast downstream motion (a jet) and a looping motion (a vortex). The trajectory of the move is the solution of the

following equations [8]:

$$\dot{x} = -\partial_y \psi(x,y,t), \quad \dot{y} = \partial_x \psi(x,y,t)$$

where $\psi(x,y,t) = -\tanh\left[\frac{y - B(t)sin(k(x-ct))}{\sqrt{1+k^2B^2(t)\cos^2(k(x-ct))}}\right]$.

Fig. 1 (Fig. 1 in [8]) shows the water motion of the meandering model. Notice that this model is deterministic. When the initial position of a sensor node is determined, its subsequent route is also determined.

In this paper, we further introduce a simpler ring-like model that consists of both local variety and main circulation, which captures some characteristics of a wider range of water bodies.

For the local variety, we use a random walk model. Formally, let a sensor node be in the cell (ox, oy). The probability that the node will be in cell (x, y) at next time slot is:

$$P_{local}((x,y)|(ox,oy)) = \begin{cases} \frac{1}{(2V_u+1)^2} & |x-ox| + |y-oy| \le V_u \\ 0 & otherwise \end{cases} \tag{4}$$

For the main circulation effects, we consider the strength and speed of the flow. This depends on specific characteristics of different sea. We illustrate with an example of Lake Pontchartrain [19] (see Fig. 2 (a)). Mainly caused by the wind in that region, its flow shows a ring-like pattern (see Fig. 2 (b)). Thus, we model it as:

$$P_{main}((x,y) \mid (ox,oy)) = \begin{cases} 1 & x = ox + \Delta_x(ox,oy) \\ & \& \ y = oy + \Delta_y(ox,oy) \\ 0 & otherwise \end{cases} \tag{5}$$

The overall U-Mobility is a combination of these two models. We use factor α and β to represent the weights of two walk model separately. Formally,

$$\begin{aligned} P((x,y) \mid (ox,oy)) \quad = \quad & \alpha \times P_{main}((x,y)|(ox,oy)) \\ & + \beta \times P_{local}((x,y)|(ox,oy)) \end{aligned} \tag{6}$$

We admit that this is a simplified U-Mobility model for ring like circulation. This selection is because 1) we believe that the ring-like model captures some major characteristics of the wave flow; 2) the ring-like model is a randomized model in contrast to the deterministic meandering model. This makes the design and analysis of the C-Mobility of the mobile sensors more comprehensive; 3) a more complex model may defeat a clear presentation of the main topic of this work.

In this paper, our C-Mobility model is designed such that it can integrate different U-Mobility models; and we will test both these two U-Mobility models.

V. Sea Surface Coverage: Design and Optimization

A. Algorithm Outline

In our algorithm, each sensor node has to maintain two types of information. First, the set of cells that it needs to cover at the end of the period. Second, the location that it has to travel to so as to cover these cells. Formally, let D_i be the set of cells that node i need to cover. We name it the *dominating set*. By our assumption, I is fully covered by sensor nodes at time 0:

$$\bigcup_{1 \le i \le n} D_i^0 = I \tag{7}$$

For a dominating set D_i, a *target cell* is the location to move to at the end of a period, so that node i can cover D_i. Notice that this location must be feasible according to its velocity constraint and the flow speed. We propose the definition of a *feasible target cell* as follows:

Definition 2: Assume at time t, the dominating set that sensor node i (in location (ox_i^t, oy_i^t)) maintains is D_i. A target cell (qx, qy) is called *feasible* if and only if the node can reach (qx, qy) before the end of period (T time slot in worst case) and cover D_i in (qx, qy):

$$\begin{aligned} & (V_c - V_u) \times (\lceil \tfrac{t}{T} \rceil T - t + 1) \ge |ox_i^t - qx| + |oy_i^t - qy| \\ & \forall \ (px,py) \in D_i, \sqrt{(px-qx)^2 + (py-qy)^2} \le R_s \end{aligned} \tag{8}$$

Usually there are many feasible target cells for node i. The *closest* feasible target cell is the one that is reachable with the least among of energy for node i. We temporarily delay the explanation of how the least energy is calculated (which will be detailed in next section). Intuitively, it is a shortest path with consideration of U-Mobility.

Obviously, a node does not need to move immediately when it finds a feasible target cell given enough time slots left. We define the status of a node to be "IDLE" or "BUSY" to indicate whether the node has to start C-Mobility.

Definition 3: Assume at time t, sensor node i in location (ox_i^t, oy_i^t) finds a feasible target cell (qx, qy). We call node i "BUSY" if and only if the following inequality holds, and "IDLE" otherwise:

$$(V_c - V_u) \times (\lceil \frac{t}{T} \rceil T - t) < |ox_i^t - qx| + |oy_i^t - qy| + V_u \tag{9}$$

Inequality (9) indicates that if node i does not move in C-Mobility at current time slot t there will not be enough time for it to move to the target cell. Thus, node i should be set as "BUSY" and start to move. Otherwise, the sensor node just take a greedy approach to stay "IDLE".

In every time slot, both the dominating set D_i of and the feasible target cell of node i will change; either because of the U-Mobility or with the collaboration of other sensor nodes. We would like to emphasize that these change does not necessarily result in C-Mobility. Intrinsically, the sensor nodes monitor the effect of U-Mobility. They negotiate with other nodes and estimate the future U-Mobility given certain U-Mobility models so as to find a collective most efficient strategy to cover the points of interest at the end of T.

Algorithm 1 Operation of Sensor Node i

```
Initialize dominate set D_i^0 and energy e_i^0
t ⇐ 0
while e_i^t > 0 do
    Update D_i^t by corporation with neighbor nodes;
    Find the closest feasible target cell for C-Mobility;
    Move in U-Mobility and C-Mobility;
    t ⇐ t + 1
end while
```

The above distributed algorithm is executed at each sensor node. We can interpret it in the following way. At every time

slot, a node first searches for the possible advantage of U-Mobility (updating its dominating set with neighboring nodes); it then computes the best way to take this advantage (finding a closest feasible target cell); and finally, the node predicts the advantage of U-Mobility in future and starts C-Mobility if necessary. The remaining task is to show the detailed designs of each step, such that the U-Mobility is better exploit and the energy consumption is balanced. We detail these designs in next section.

B. Updating Dominating Set

The objective of updating dominating set is to hold the coverage after the U-Mobility so that each point of interest will be dominated by a sensor node. The dominating set of a sensor node can change when this sensor is floating away by the U-Mobility. It can also change because that this sensor *inherits* the coverage responsibility from other nodes; or hands its coverage responsibility to other nodes. The sensor nodes update the coverage responsibility with neighboring nodes with concerns of residual energy.

In this paper, we call two nodes to be neighbors if they are within each other's communication range R_c. Assume point $(px, py) \in D_i^t$ is covered by node i at time slot t, there are two different cases to update D_i^t:

CASE I: Let j be a neighbor of node i. If the status of node j is "BUSY" and its target cell (qx_j, qy_j) is within the sensing range of (px, py), point (px, py) could be removed from D_i^t and added into D_j^t.

We select the node j which best fit for load balance. Formally, let $\mathcal{B}$ be the set of nodes that satisfies this condition,

$$\begin{aligned} &maximize \;\; e_j^t, j \in \mathcal{B} \\ &s.t.\ (1)\ node\ j\ is\text{``}BUSY\text{''} \\ &\quad (2)\ \sqrt{(ox_j - ox_i)^2 + (oy_j - oy_i)^2} \le R_c \\ &\quad (3)\ \sqrt{(qx_j - px)^2 + (qy_j - py)^2} \le R_s \end{aligned} \tag{10}$$

This problem can be solved optimally by a greedy algorithm; and we choose the one with the maximum residual energy to inherit (px, py) from node i as shown in Equ. (10).

In this case, node j does not need to pay anything to inherit (px, py). However, such neighbor node may not be available. In more general situations, a node has to change its target cell to inherit the coverage of (px, py).

CASE II: Let j be a neighbor of node i. Define dominating set D_j^{t+} as:

$$D_j^{t+} = D_j^t \cup \{(px, py)\} \tag{11}$$

If the closest feasible target cell (qx_j^+, qy_j^+) for D_j^{t+} to (ox_j, oy_j) exists at the beginning of time slot t, node j is able to inherit the coverage of (px, py) from node i.

For a node j whose dominating set has (px, py), define dominating set D_j^{t-} as:

$$D_j^{t-} = D_j^t \setminus \{(px, py)\} \tag{12}$$

Obviously a feasible target cell (qx_j^-, qy_j^-) for D_j^{t-} exists. The difference between selecting (qx_j^+, qy_j^+) or (qx_j^-, qy_j^-) is the extra cost that node j needs to pay if it decide to inherit the coverage of (px, py) from node i.

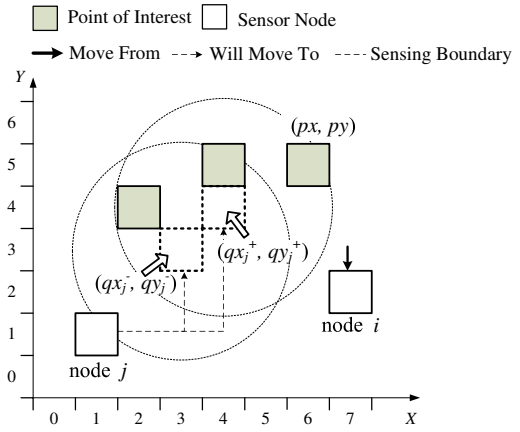

Fig. 3. Node j can adjust its target cell to cover (px, py)

Figure. 3 illustrates CASE II by an example. Node i moves from $(7, 3)$ to $(7, 2)$ and loses the coverage of the point of interest $(px, py) = (6, 5)$. Node j has the dominating set $D_j^{t-} = \{(2, 4), (4, 5)\}$ and the corresponding target cell is $(qx_j^-, qy_j^-) = (3, 3)$ which can not cover $(px, py) = (6, 5)$. Node j can adjust its target cell to $(qx_j^+, qy_j^+) = (4, 4)$ to cover the original points of interest from D_j and (px, py) at the same time. Thus, node j is a potential node that could inherit (px, py) from node i but it may need to take more steps to move to the new target cell.

There might be many potential nodes which could inherit the coverage of (px, py); and they have different costs. Let $f_{ox,oy}(qx, qy)$ denote the energy cost for a node to move from (ox, oy) to target cell (qx, qy) (we will introduce how to calculate f in next section). For every potential node j, the extra energy cost to inherit coverage of (px, py) is:

$$\triangle_j = f_{ox_j, oy_j}(qx_j^+, qy_j^+) - f_{ox_j, oy_j}(qx_j^-, qy_j^-) \tag{13}$$

Again, we choose the node with the maximum residual energy that is deducted by $\triangle$ for load balancing purpose:

$$\begin{aligned} &maximize \;\; (e_j^t - \triangle_j) \\ &s.t.\ (1)\ \sqrt{(ox_j - ox_i)^2 + (oy_j - oy_i)^2} \le R_c \\ &\quad (2)\ \exists\ (qx_j^+, qy_j^+),\ (qx_j^+, qy_j^+)\ is\ the \\ &\qquad closest\ feasible\ target\ cell\ for\ D_j^{t+} \end{aligned} \tag{14}$$

Obviously node $j = i$ is one of the potential nodes which can inherit (px, py) from node i. Therefore, solution exists in CASE II. It can be guaranteed that at every time slot the union of the dominate sets is I, as shown in Lemma 1.

Lemma 1: At every time slot t, the union of the dominating sets D_i^t from all sensor nodes equals to the set of points of interest I:

$$\forall t \ge 0, \quad \bigcup_{1 \le i \le n} D_i^t = I \tag{15}$$

Proof: For $t = 0$, it holds based on the problem assumption in Equ. (7). Assume the lemma holds for $t = k$:

$$\bigcup_{1 \le i \le n} D_i^k = I$$

For $t = k + 1$, $\forall\ i$, $\forall\ p \in D_i^k$, p will be either in D_i^{k+1} or D_j^{k+1} while node j is selected by the approach above

according to the process of "updating dominating set". Thus, we have:

$$\bigcup_{1\le i\le n} D_i^{k+1} = \bigcup_{1\le i\le n} D_i^k = I \tag{16}$$

The lemma holds by induction. ■

C. Find the Closest Feasible Target Cell

Every time a sensor node updates its dominating set, or the current location of this sensor node is changed, it needs to recalculate the feasible target cells that it should move to for covering this dominating set. The objective is to find the feasible target cell that is optimized in terms of moving distance from its current location to this target cell.

We have on purposely delayed the description of the *closest* feasible target cell. If there is no U-Mobility, or the pattern of U-Mobility is entirely unknown, we use the shortest path from (ox, oy) to (qx, qy) as the estimated energy cost for the weights of the feasible target cells:

$$f_{ox,oy}(qx, qy) = |qx - ox| + |qy - oy| \tag{17}$$

However, different U-Mobility patterns may seriously affect the weight of the path and the selection of the target cell. Let $(\overline{U_x}(x,y), \overline{U_y}(x,y))$ denote the expected cell that the node will move from (x, y) in one time slot under a U-Mobility pattern. Given this $\overline{U}$, we construct a weighted direct graph $G(V, E, W)$ such that:

$$\begin{array}{ll} V & = \{v_i = (x_i, y_i) \mid cell\ (x_i, y_i)\ in\ the\ region\} \\ E & = \{(v_i, v_j) \mid |x_j - \overline{U_x}(x_i, y_i)| + |y_j - \overline{U_y}(x_i, y_i)| \le V_c\} \\ W & = \{w_{ij} \ = \ |x_j - \overline{U_x}(x_i, y_i)| + |y_j - \overline{U_y}(x_i, y_i)|\} \end{array} \tag{18}$$

If the U-Mobility is known in advance and shows a long term behavior, the shortest path between any pair of two cells are calculated at the initial stage in graph $G(V, E, W)$. In our simulation, we will see the effect of the two U-Mobility models discussed in Section IV.

D. Move in U-Mobility and C-Mobility

After finding the closest feasible target cell, a node may start to move. We would like to clarify that the closet feasible target cell is a macro target but it is usually not reachable in one time slot. After each time slot the status (the dominating set and the closest feasible target cell) of the sensor node can change. In local movement, the sensor node still can take advantage of the U-Mobility on the fly.

CASE I: If node i is "IDLE" at time t, it only moves in U-Mobility. The energy cost of node i for this time slot is zero: $e_i^{t+1} = e_i^t$.

CASE II: If node i is "BUSY" at time t, it will move both in U-Mobility and C-Mobility.

Let tx_i^t and ty_i^t be the number of steps that node i will move along X-axis and Y-axis separately in C-Mobility during this time slot. After C-Mobility, at the end of time slot t (or beginning of time slot $t+1$), we could obtain the new position of node i by:

$$\begin{cases} ox_i^{t+1} & = U_x(ox_i^t, oy_i^t) + tx_i^t \\ oy_i^{t+1} & = U_y(ox_i^t, oy_i^t) + ty_i^t \end{cases} \tag{19}$$

Intuitively, we prefer to select such a pair of (tx_i^t, ty_i^t) that could minimize the total cost of energy moving from (ox_i^t, oy_i^t) to (qx_i^t, qy_i^t). Meanwhile, (tx_i^t, ty_i^t) should not exceed the maximum velocity of V_c and guarantee node i could reach the target cell in time after this C-Mobility:

$$\begin{array}{l} minimize\ (|tx_i^t| + |ty_i^t| + f_{ox_i^{t+1}, oy_i^{t+1}}(qx_i^t, qy_i^t)) \\ s.t.\ (1)\ |tx_i^t| \ + \ |ty_i^t| \ \le \ V_c \\ \quad (2)\ (qx_i^t, qy_i^t)\ is\ still\ a\ feasible\ target\ cell \\ \quad\quad at\ the\ beginning\ of\ time\ slot\ \text{t+1} \end{array} \tag{20}$$

Condition (1) in Equ. (20) indicates the velocity constraint of C-Mobility while condition (2) guarantees the node could arrive at the target cell in time with this C-Mobility. Once the shortest path on $G(V, E, W)$ is found, (tx, ty) could be determined by the subsequent node on the shortest path. We also notice that CASE I is actually a special case for CASE II while $(tx, ty) = (0, 0)$ is a best solution.

Lemma 2: At the end of every time t, for every node i, there exists a feasible target cell (qx_i, qy_i) for D_i^t.

Proof: We just need to prove that there exists at least one pair of (tx_i^t, ty_i^t) which satisfies the conditions in Equ. (20) so that (qx_i^t, qy_i^t) is a feasible target cell at the beginning of time slot $t + 1$ (the end of time slot t).

Let $x' = U_x(ox_i^t, oy_i^t)$ and $y' = U_y(ox_i^t, oy_i^t)$, according to the maximum velocity of U-Mobility, we could obtain:

$$\begin{array}{ll} & |ox_i^t - x'| + |oy_i^t - y'| \le V_u \\ \Rightarrow & -V_u \le (|qx_i^t - ox_i^t| - |qx_i^t - x'|) + \\ & \quad (|qy_i^t - oy_i^t| - |qy_i^t - y'|) \le V_u \end{array} \tag{21}$$

We have two different cases to analyze:

1) If $|x' - qx_i^t| + |y' - qy_i^t| \le V_c$

Let $tx_i^t = qx_i^t - x'$ and $ty_i^t = qy_i^t - y'$ which could satisfy the velocity constraint of C-Mobility.

$$\begin{array}{ll} & |ox_i^{t+1} - qx_i^t| + |oy_i^{t+1} - qy_i^t| \\ = & |x' + tx_i^t - qx_i^t| + |y' + ty_i^t - qy_i^t| \\ = & |x' + (qx_i^t - x') - qx_i^t| + |y' + (qy_i^t - y') - qy_i^t| \\ = & 0 \\ \text{thus} & (V_c - V_u) \times (\lceil \frac{t+1}{T} \rceil T - (t+1) + 1) \ge \\ & \quad |ox_i^{t+1} - qx_i^t| + |oy_i^{t+1} - qy_i^t| = 0 \end{array} \tag{22}$$

In this case, we have a solution $(tx_i^t, ty_i^t) = (qx_i^t - x', qy_i^t - y')$ to guarantee (qx_i^t, qy_i^t) is a feasible target cell at the beginning of time slot $t + 1$.

2) If $|x' - qx_i^t| + |y' - qy_i^t| > V_c$

In this case, there must exists a pair of value (x^*, y^*) so that:

$$\begin{array}{l} (a)\ minof(x', qx_i^t) \le x^* \le maxof(x', qx_i^t) \\ (b)\ minof(y', qy_i^t) \le y^* \le maxof(y', qy_i^t) \\ (c)\ |x^* - x'| + |y^* - y'| = V_c \end{array} \tag{23}$$

Let $tx_i^t = x^* - x'$ and $ty_i^t = y^* - y'$, we could obtain:

$$\begin{array}{ll} & (|qx_i^t - ox_i^t| + |qy_i^t - oy_i^t|) - \\ & \quad (|qx_i^t - ox_i^{t+1}| + |qy_i^t - oy_i^{t+1}|) \\ = & (|qx_i^t - ox_i^t| - |qx_i^t - x'| - |ox_i^{t+1} - x'|) + \\ & \quad (|qy_i^t - oy_i^t| - |qy_i^t - y'| - |oy_i^{t+1} - y'|) \\ = & |qx_i^t - ox_i^t| - |qx_i^t - x'| + |qy_i^t - oy_i^t| - |qy_i^t - y'| + V_c \\ \ge & V_c - V_u \qquad\qquad from\ (21) \end{array} \tag{24}$$

Since (qx_i^t, qy_i^t) is feasible at the beginning of time slot t, we have:

$$(V_c - V_u) \times (\lceil \frac{t}{T} \rceil T - t + 1) \geq |ox_i^t - qx_i^t| + |oy_i^t - qy_i^t| \quad (25)$$

Meanwhile, it is easy to get:

$$\begin{aligned} &(V_c - V_u) \times (\lceil \tfrac{t}{T} \rceil T - t + 1) - \\ &(V_c - V_u) \times (\lceil \tfrac{t+1}{T} \rceil T - (t+1) + 1) \leq V_c - V_u \end{aligned} \quad (26)$$

Combine three inequalities above, we could achieve:

$$(V_c - V_u) \times (\lceil \frac{t+1}{T} \rceil T - (t+1) + 1) \geq |qx_i^t - ox_i^{t+1}| + |qy_i^t - oy_i^{t+1}| \quad (27)$$

Therefore, in both two cases, we could obtain a solution pair of (tx_i^t, ty_i^t) which satisfies the constraints in Equ. (20). At the end of every time slot, for any node there exists a feasible target cell. ■

As the sensor network is able to collectively hold the dominating sets and each sensor node is able to find feasible target cell to move to maintain the dominating set, the coverage is guaranteed, as proved by the following theorem.

Theorem 3: At the end of every T time slot, every point of set of points of interest I is covered by a sensor.

$$\begin{aligned} &\forall k \geq 0, \forall (px, py) \in I, \exists u, 1 \leq u \leq N \\ &s.t. \sqrt{(px - ox_u^{kT})^2 + (py - oy_u^{kT})^2} \leq R \end{aligned} \quad (28)$$

Proof: At the end of every time slot kT, for any point of interest $p \in I$, we know that $\exists\ u,\ p \in D_u^{kT}$ from Lemma 1. For the dominating set D_u^{kT}, according to Lemma 2, there exists a feasible target cell (qx_u, qy_u) which satisfies:

$$\begin{aligned} &(i) \quad \sqrt{(qx_u - px)^2 + (qy_u - py)^2} \leq R_s \\ &(ii) \quad (V_c - V_u) \times (\lceil \tfrac{kT+1}{T} \rceil T - kT) \\ &\qquad \geq |ox_u^{kT} - qx_u| + |oy_u^{kT} - qy_u| \\ &\Rightarrow \quad (V_c - V_u) \times 0 \geq |ox_u^{kT} - qx_u| + |oy_u^{kT} - qy_u| \\ &\Rightarrow \quad |ox_u^{kT} - qx_u| + |oy_u^{kT} - qy_u| = 0 \\ &\Rightarrow \quad ox_u^{kT} = qx_u,\ oy_u^{kT} = qy_u \end{aligned} \quad (29)$$

Combine (i) and (ii), we can achieve that point of interest p is in the sensing range of node u. ■

VI. The Distributed Protocol

In previous section, we have detailed the SSC algorithm. To realize this algorithm, there are many practical difficulties to address. Most importantly, as the algorithm requests distributed maintenance of the dominating sets, different nodes will have different views due to the latency of communication. More specifically, if node A finds that node C is able to inherit a point of interest P_A and node B also finds that C is able to inherit a point of interest P_B, there is a *collision* as node C may not inherit P_A, P_B simultaneously. We develop a distributed protocol to address such practical issues.

In our distributed protocol, every sensor node maintains a local information table as shown in Table. I:

TABLE I
Local Information Table on Node

Name	Description
D	Dominating set
(ox, oy)	Current location
(qx, qy)	Target cell to reach at the end of next T time slot
(tx, ty)	Temporary target in current time slot

The current location (ox, oy) of a sensor node is obtained by GPS or other mechanisms at the beginning of every time slot. For (qx, qy) and (tx, ty), one may consider their relationship to be that (qx, qy) is the final destination at the end of the period T and (tx, ty) is the next hop. Notice, however, that (qx, qy) is also changing if D changes.

To avoid the collision in updating dominating set, each node works as follows:

1) Node i broadcasts a $Query$ message to its one-hop neighbor nodes to claim that it is querying for some node to take the responsibility to cover (px, py):

$$i \Rightarrow\ neighbors \quad Query \mid i \mid (px, py) \quad (30)$$

2) Node j receives this $Query$ message and finds that it is possible to add (px, py) in its dominating set D_j. Then, node j sends a $Response$ message back to node i with the status of node j and the cost to inherit (px, py):

$$\begin{aligned} j \Rightarrow\ i \quad & Response \mid j \mid (px, py) \mid \\ & status \mid evaluating\ value \end{aligned} \quad (31)$$

3) For all the $Response$ node i receives, it ranks the candidates according to the cost metric defined in section V. Node i will then send a $Request$ message to request a node in the candidate list in order to inherit (px, py):

$$i \Rightarrow\ j \quad Request \mid i \mid (px, py) \quad (32)$$

4) After receiving a $Request$ message, node j will make a decision based on current dominating set to see whether it can accept this request (e.g., if node j has accepted a request from other node at this time, the dominating set maybe changed so the re-judgement is necessary) and send a feedback to node i:

$$\begin{aligned} j \Rightarrow\ i \quad & Req\_Accept \mid j \mid (px, py) \\ j \Rightarrow\ i \quad & Req\_Reject \mid j \mid (px, py) \end{aligned} \quad (33)$$

Node i will send requests to the nodes in candidate list until a $Request\_Accept$ is received or the end of the list is reached.

We will evaluate our protocol and show that it has a low average communication overhead by simulation.

VII. Performance Evaluation

A. Simulation Settings

We evaluate our SSC in an event driven simulator. The default values of our simulation are as follows. We deploy 500 sensor nodes in a region of $500m \times 500m$ for the random ring model, and $1600m \times 400m$ for the meandering model. Each cell for computation is a square of $5m \times 5m$. In both models, 1000 points of interest are randomly and uniformly distributed in the region. For the mobile sensor nodes, the sensing range is $R_s = 50m$ and the default communication range $R_c = 100m$. We adopt the movement parameters similar to Starbug AUV [10]. The maximum speed of Starbug is 1.5m/s (3 knots), i.e., $V_c = 1.5m/s$. The battery allows a continuous movement for a distance of 7500m. The maximum velocity of U-Mobility is $V_u = 0.5m/s$ [8]. We set one time slot as 100 seconds (e.g. $t = 100s$) and time interval $T = 10t$. The system lifetime is the first sensor node that the energy is depleted. We use the standard deviation $\sigma(t)$ of the residual energy to represent the energy balance among sensors at time t.

$$\sigma(t) = \sqrt{\frac{1}{N}\sum_{i=1}^{N}(e_i^t - \overline{e^t})^2} \quad (34)$$

We evaluate both the meandering model and the random ring model for U-Mobility. The simulation results are the average of 10 randomly conducted experiments.

B. Network Lifetime and Balance of Energy

We first compare the SSC to the back-to-original reposition scheme that we presented in Section III.B under random ring model. We evaluate our SSC in two communication range settings, i.e., $100m$ and $200m$ (notice that the sensing range does not change). In Fig. 4, Y-axis is the minimal residual energy of the sensor nodes in the network. It is normalized to represent the remaining distance a node can travel. Clearly, the minimum energy of the back-to-original scheme decreases much faster and the system lifetime is only around $25 \times 10^3 s$. Our SSC algorithm has a system lifetime of $90 \times 10^3 s$, a more than three-time improvement. If the communication range is $200m$, the lifetime is improved further to $180 \times 10^3 s$, i.e., around 45 hours.

Fig. 5 illustrates that SSC better balances the residual energy of the sensor nodes. The standard deviation of the residual energy is very small compared with the back-to-original scheme. More interestingly, as time evolves, the increase of the standard deviation almost flattened. This shows that our SSC is able to scale better. This is further verified by Fig. 6, where we show the distribution of the residual energy at the end of the system lifetime. We can see that the residual energy of most sensor nodes can only support a traveling distance of less than 1000 meters in SSC, i.e., less than 15% of the energy reserve. As a comparison, in the back-to-original scheme, many sensor nodes have significant residual energy left.

C. Communication Range and Overhead

We see in Fig. 7, the system lifetime increases as the communication range increases. This is because that the sensor nodes are able to find more neighboring nodes and make better decisions. When the communication range is above $200m$, however, improvement is marginal. It is not surprising as the sensing range and velocity of a sensor node have a limit. Therefore, seeking help from sensors that are far away is not helpful. This locality property strongly support our distributed protocol design against a design of overall optimization.

Though we neglect the communication cost in the design of C-Mobility, we evaluate the communication overhead of our protocol as large overhead will affect the protocol latency and increase packet collisions and retransmission. There are five main types of packets in our protocol: *Query*, *Response*, *Request*, *Req_Accept* and *Req_Reject*. From Fig. 8, we can see that there is a bell shape for the number of packets generated during each time period T. During the initial period the sensor nodes are losing their positions and are more and more aggressively negotiating with the candidate nodes that can exchange the dominating set. After that, the number of "BUSY" nodes increases and less dominating set updates happens as compared with the "IDLE" state. Notice that every time $T = 10t$, the number of communication packets become zero which indicates no dominating set update happens. From another point of view, this verifies that our scheme guarantees the coverage. Fig. 8 shows that every node results less than 100 packets totally in one time slot. Since each time slot represents $100s$, this is a very low communication requirement.

We compare the overhead of different communication range in Fig. 9. When the communication range doubles, we see that the overhead increases less than 4 times. This clearly shows the scalability of our protocol.

Fig. 10 compares the ratio of *Request* and *Query*. This indicates the number of collisions in each query. As we can see, the ratio is less than 1.5; this means that most nodes can find a proper node to inherit that cell by the first try.

D. Meandering Model

We then evaluate SSC for meandering current model. We see from Fig. 11 that though not as significant as the random ring model, SSC shows greatly increased (50% and 150% for two different CR respectively) lifetime than back-to-original scheme. From Fig. 12, we also see that SSC balance the energy consumption better. By looking into the details of the simulation data trace, we observe that the meandering model shows a much more deterministic jet behavior. All the sensor nodes are pushed more consistently in one direction. This makes the benefit of exploring the U-Mobility less significant. Considering an extreme case where all the sensor nodes are pushed straight towards one direction, then SSC will reduce to back-to-original as the sensor nodes have no choice other than going back. Nevertheless, our simulation results have clearly shown that exploiting the benefit of the U-Mobility.

VIII. Conclusion

In this paper, we for the first time study a double mobility coverage problem for sea surface monitoring. Our problem is sharply different from previous works as we face both an uncontrollable mobility by the sea flows and a controllable mobility of the sensor nodes. We made an observation that U-mobility not only breaks the coverage of the sensor network but also sends the sensor nodes to the locations that may improve the coverage. Thus, the key target of this paper is by leveraging U-Mobility, to minimize the movement distance in C-Mobility and balance the energy consumption among all the sensor nodes to provide a guaranteed coverage of the points of interest. We proposed a distributed sea surface coverage (SSC) algorithm which leverage the advantage of the U-Mobility. The algorithm naturally addressed a set of difficulties, such as the limitation of the velocity of the mobile sensor nodes, and the balance of energy consumption. We proved that the algorithm guarantees coverage. A distributed protocol was then developed that addressed a set of practical concerns, e.g., competition of transferring the coverage responsibility to other nodes. Our simulation results demonstrated that SSC can extend the system lifetime over a back-to-original scheme under various configurations significantly.

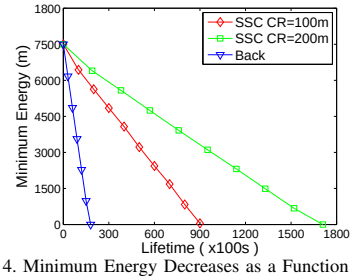

Fig. 4. Minimum Energy Decreases as a Function of Time (U-Mobility: Random Ring Model)

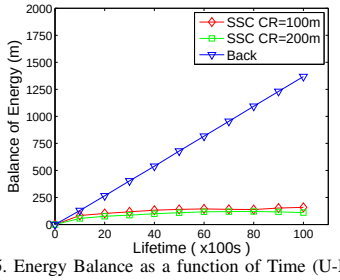

Fig. 5. Energy Balance as a function of Time (U-Mobility: Random Ring Model)

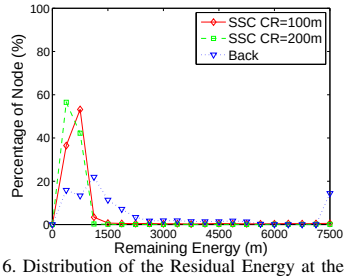

Fig. 6. Distribution of the Residual Energy at the End of System Lifetime (U-Mobility: Random Ring Model)

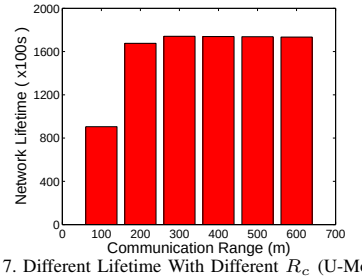

Fig. 7. Different Lifetime With Different R_c (U-Mobility: Random Ring Model)

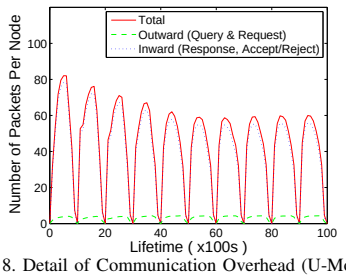

Fig. 8. Detail of Communication Overhead (U-Mobility: Random Ring Model)

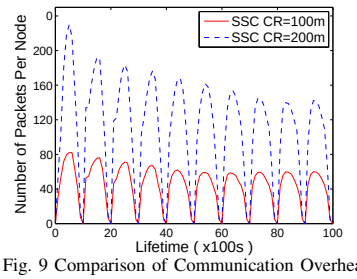

Fig. 9 Comparison of Communication Overhead (U-Mobility: Random Ring Model)

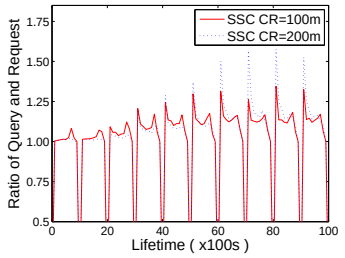

Fig. 10. Ratio of *Query* and *Request* (U-Mobility: Random Ring Model)

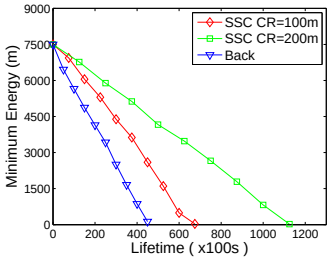

Fig. 11. Minimum Energy Decreases as a Function of Time (U-Mobility: Meandering Model)

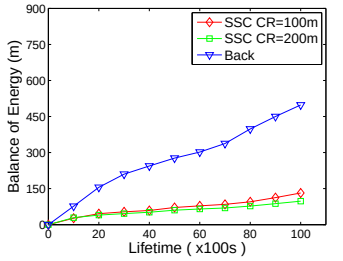

Fig. 12. Energy Balance as a function of Time. Y-axis represents the standard deviation (U-Mobility: Meandering Model)

ACKNOWLEDGMENTS

The research was supported in part by grants from RGC under N HKUST609/07, by grant from HKUST under MRA05/06.EG03, by grant from National Basic Research Program of China (973 Program) under No. 2006CB303000, the NSFC oversea Young Investigator grant under No. 60629203, National 863 Program of China under No. 2006AA01Z228; by grant from HKPU under ICRG G-YG78, A-PB0R, and RGC under GRF PolyU 5305/08E.

REFERENCES

[1] Autonomous Ocean Sampling Network, http://www.mbari.org/aosn/

[2] MBARI drifters, http://www.mbari.org/muse/platforms/drifters.htm.

[3] Lake Illawarra Authority - Lake Facts: Tides and Currents. http://www.lia.nsw.gov.au/facts/tides_and_currents.html

[4] UAM Moorings, http://www.mbari.org/muse/platforms/UAM-mooring.html.

[5] E. Smith, et al., Satellite-Derived Sea Surface Temperature Data Available From the NOAA/NASA Pathfinder Program, http://www.agu.org/eos_elec/95274e.html

[6] I. Akyildiz, D. Pompili, and T. Melodia, "Underwater Acoustic Sensor Networks: Research Challenges", in *Ad Hoc Networks*, vol. 3, no. 3, pp. 257-279, Mar. 2005.

[7] G. Werner-Allen, K. Lorincz, J. Johnson, J. Lees, and M. Welsh, "Fidelity and Yield in a Volcano Monitoring Sensor Network", in *Proc. USENIX OSDI'06*, Seattle, WA, Nov. 2006.

[8] A. Caruso, F. Paparella, L. Vieira, M. Erol, and M. Gerla, "The Meandering Current Mobility Model and Its Impact on Underwater Mobile Sensor Networks", in *Proc. IEEE INFOCOM'08*, Phonix, AZ, Apr. 2008.

[9] X. Du and F. Lin, "Improving Sensor Network performance by Deploying Mobile Sensors", in *Proc. the 24th IEEE International Performance, Computing and Communications Conference*, Pheonix, AZ, Apr. 2005.

[10] M. Dunbabin, J. Roberts, K. Usher, G. Winstanley, and P. Corke, "A Hybrid AUV Design for Shallow Water Reef Navigation", in *Proc. IEEE ICRA'05*, Barcelona, Spain, Apr. 2005.

[11] C. Ebbesmeyer, C. Coomes, V. Kolluru, and E. Edinger, "Net Water Movement in Budd Inlet: Measurements and Conceptual Model", in *Proc. Puget Sound Research Conference*, Seattle, WA. Mar. 1998.

[12] W. Heinzelman, A. Chandrakasan, and H. Balakrishnan, "Energyefficient communication protocol for wireless microsensor networks," in *Proc. HICSS'00*, Maui, Hawaii, Jan., 2000.

[13] A. Howard, M. Mataric and G. Sukhatme, "Mobile Sensor Network Deployment Using Potential Field: a distributed scalable solution to the area coverage problem", in *Proc. International Conference on Distributed Autonomous Robotic Systems'02*, June. 2002.

[14] S. Kim, S. Pakzad, D. Culler, J. Demmel, G. Fenves, S. Glaser, and M. Turon, "Health Monitoring of Civil Infrastructures Using Wireless Sensor Networks", in *Proc. ACM IPSN'07*, Cambridge, MA, Apr. 2007.

[15] S. Kumar, T. Lai, J. Balogh, "On k-coverage in a mostly sleeping sensor network", in *Proc. ACM MOBICOM'04*, Philidephia, PA, Sept. 2004.

[16] B. Liu, P. Brass, O. Dousse, P. Nain, and D. Towsley, "Mobility improves coverage of sensor networks", in *Proc. MOBIHOC'05*, Urbana-Champaign, IL, 2005.

[17] J. Pedlosky, Ocean Circulation Theory. Heidelberg: Springer-Verlag, 1996.

[18] G. Sibley, M. Rahimi and G. Sukhatme, "Robomote: A Tiny Mobile Robot Platform for Large-Scale Sensor Networks," in *Proc. IEEE ICRA'02*, Washington D.C., May, 2002.

[19] R. Signell and J. List, "Modeling Waves and Circulation in Lake Pontchartrain", Gulf Coast Association of Geological Societies Transactions, vol. 47, pp. 529-532, 1997.

[20] D. Wang, Q. Zhang, and J. Liu, "Partial Network Coding: Theory and Application for Continuous Sensor Data Collection", in *IEEE IWQoS'06*, New Haven, CT, 2006.

[21] D. Wang, J. Liu, and Q. Zhang, "Field Coverage using a Hybrid Network of Static and Mobile Sensors", in *IEEE IWQoS'07*, Chicago, IL, 2007.